Available online at www.sciencedirect.com
SCIENCE DIRECT®
Bioorganic & Medicinal Chemistry Letters 15 (2005) 1429–1433
Bioorganic & Medicinal Chemistry Letters

Synthesis and SAR of 4-(3-hydroxyphenylamino)pyrrolo-[2,1-*f*][1,2,4]triazine based VEGFR-2 kinase inhibitors

Robert M. Borzilleri,[a] Zhen-wei Cai,[a] Christopher Ellis,[a] Joseph Fargnoli,[b] Aberra Fura,[c] Tracy Gerhardt,[b] Bindu Goyal,[a] John T. Hunt,[a] Steven Mortillo,[b] Ligang Qian,[a] John Tokarski,[d] Viral Vyas,[c] Barri Wautlet,[b] Xioping Zheng[a] and Rajeev S. Bhide[a,*]

[a]*Departments of Oncology Chemistry, Bristol-Myers Squibb Pharmaceutical Research Institute, Princeton, NJ 08543-4000, USA*
[b]*Departments of Oncology Drug Discovery, Bristol-Myers Squibb Pharmaceutical Research Institute, Princeton, NJ 08543-4000, USA*
[c]*Departments of Metabolism and Pharmacokinetics, Bristol-Myers Squibb Pharmaceutical Research Institute, Princeton, NJ 08543-4000, USA*
[d]*Departments of Structural Biology and Modeling, Bristol-Myers Squibb Pharmaceutical Research Institute, Princeton, NJ 08543-4000, USA*

Received 2 December 2004; revised 23 December 2004; accepted 30 December 2004
Available online 22 January 2005

Abstract—A versatile synthesis of the suitably functionalized pyrrolo[2,1-*f*][1,2,4]triazine nucleus is described. SAR at the C-5 and C-6 positions of the 4-(3-hydroxy-4-methylphenylamino)pyrrolo[2,1-*f*][1,2,4]triazine template led to compounds with good in vitro potency against VEGFR-2 kinase. Glucuronidation of the phenol group is mitigated by incorporation of a basic amino group on the C-6 side chain of the pyrrolotriazine nucleus.

Angiogenesis, the growth and expansion of blood vessels from preexisting vasculature, is involved in a variety of disease states that include diabetic retinopathy, rheumatoid arthritis, and tumor growth.[1] Vascular endothelial growth factors (VEGF) and their cognate receptors (VEGFR), are critically involved in multiple processes of angiogenesis that include increased vascular permeability, endothelial cell (EC) migration, proliferation, and survival.[2] Of these receptors, VEGFR-2 is predominantly expressed on ECs and is involved in various aspects of tumor angiogenesis. Consequently, this receptor tyrosine kinase has become an attractive target for the treatment of multiple tumor types.[3] Positive results from the clinical trials of Bevacizumab (Avastin™), a monoclonal antibody against VEGF, demonstrated increased benefit in survival when used in combination with cytotoxic agents.[4] Accordingly, reduction in tumor growth via disruption of the VEGF pathway is a viable strategy for cancer therapy.

We recently reported the discovery of the pyrrolotriazine nucleus as a template for potent inhibitors of epidermal growth factor receptor (EGFR) and VEGFR-2 (Fig. 1).[5] In that preliminary report, the structure–activity relationships (SAR) focused on the effects of methyl substitution at the 5-, 6-, and 7-positions of pyrrolotriazines containing different C-4 aniline substituents. Herein we describe the expanded SAR studies of the 4-(3-hydroxyphenylamino)pyrrolotriazines on the inhibition of VEGFR-2 kinase activity. This paper also highlights a general synthesis of substituted C-5 and C-6 pyrrolotriazines, which provided an opportunity to improve the in vitro potency and metabolic stability of these compounds.

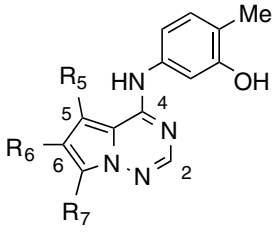

Figure 1. General structure of the pyrrolo[2,1-*f*][1,2,4]triazine based VEGFR-2 inhibitors reported previously.[5]

Keywords: VEGFR-2; Angiogenesis; SAR; Kinase receptor.
* Corresponding author. Tel.: +1 609 252 4395; fax: +1 609 252 6601; e-mail: rajeev.bhide@bms.com

0960-894X/$ - see front matter © 2005 Elsevier Ltd. All rights reserved.
doi:10.1016/j.bmcl.2004.12.079

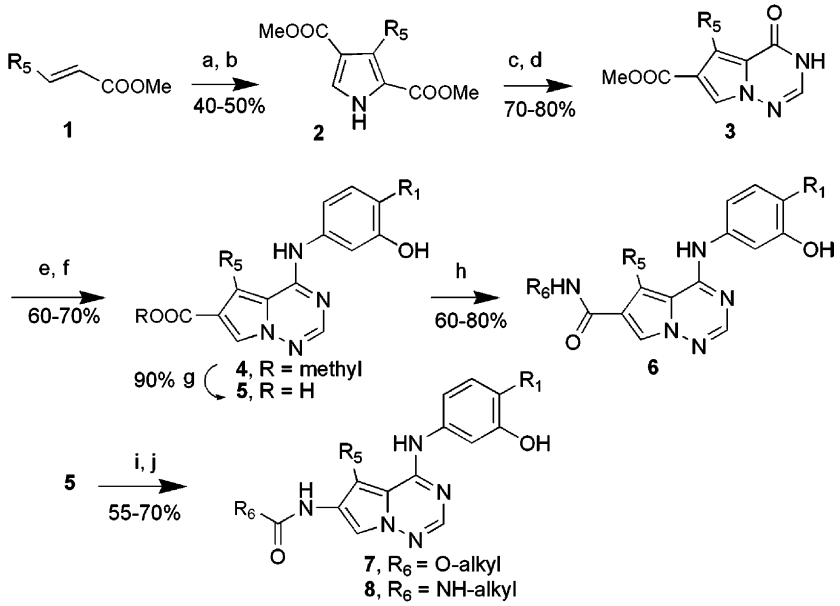

Scheme 1. Synthesis of C-6 amides, ureas, carbamates. Reagents: (a) TosMIC, sodium hydride, DMSO, THF; (b) $AlCl_3$, CCl_3COCl, then NaOMe, MeOH; (c) $Ph_2P(O)ONH_2$, NaH, DMF; (d) formamide, heat; (e) $POCl_3$, heat; (f) aniline, heat; (g) LiOH; (h) EDCI, R_6NH_2; (i) diphenylphosphoryl azide; (j) R_6OH or R_6NH_2.

Pyrrolo[2,1-*f*][1,2,4]triazine derivatives bearing carboxamides and carbamates at the C-6 position were prepared as shown in Scheme 1.[6] β-Substituted acrylates of general formula **1** were treated with tosylmethyl isocyanide (TosMIC) in the presence of sodium hydride to obtain 3,4-disubstituted pyrroles. Acylation at the C-2 position of these disubstituted pyrroles with trichloroacetyl chloride in the presence of aluminum chloride, followed by treatment with sodium methoxide afforded the tri-substituted pyrroles **2**.[7] The highly electron deficient pyrrole nitrogen of **2** was difficult to aminate with commercially available *O*-mesitylenesulfonylhydroxylamine (MSH).[5] However, N-amination occurred in high yield with diphenyl phosphoryl hydroxylamine.[8] The aminated pyrrole intermediate was heated in formamide to obtain the pyrrolotriazine nucleus **3**. Treatment of **3** with phosphorous oxychloride at elevated temperature afforded the hydrolytically-unstable chloroimidate intermediate, which when treated with an appropriately substituted aniline, provided compound **4**. The ester group at C-6 of **4** was easily manipulated to obtain various functional groups, which could be used as tethers for incorporating the desired appendages. Thus, following the hydrolysis of esters **4** with lithium hydroxide, the resulting acids **5** were coupled with amines to obtain amides **6**. The acids **5** underwent Curtius rearrangement when treated with diphenylphosphoryl azide in the presence of an appropriate alcohol or amine to afford carbamates **7** or ureas **8**, respectively.

The ester group at the C-6 position of the pyrrolotriazine **3** was converted to the C-6 ether (**13**) as shown in Scheme 2. Protection of the C-4 position of **3** as the phenyl ether was carried out by conversion of the C-4 amide group to the chloroimidate (see Scheme 1) followed by treatment with sodium phenoxide to give **9**. The ester group of **9** was converted to the aldehyde group (**10**) via a reduction-oxidation sequence. Baeyer–Villiger rearrangement of the aldehyde **10** occurred upon treatment with *m*CPBA to provide phenol **11** (R_6 = H). For compounds where R_5 = *i*-propyl, elevated temperatures were needed to effect this rearrangement.[6] Alkylation of the C-6 hydroxyl group of **11** was achieved either by Mitsunobu reaction or by treatment with an alkyl halide in the presence of a base to afford **12**. The phenol ether protecting group at C-4 of **12** was hydrolyzed with warm HCl, and the resulting amide was converted to the target compounds **13** (R_6 = alkyl) as previously described in Scheme 1.

Our initial studies had revealed that the 3-hydroxy aniline at the C-4 position of the pyrrolotriazine ring affords potent VEGFR-2 kinase inhibition,[5] and was therefore used throughout the SAR studies described in this report. A methyl group *para* to the aniline nitrogen improved potency, however increasing the size of the alkyl substituent led to a gradual decrease in potency as shown in Table 1. Electron withdrawing groups (**19**, **20**) did not improve the potency. Since the methyl group afforded the most potent compound, it was retained during the SAR studies focused at the C-5 and C-6 positions of the pyrrolotriazine core.

Alkyl groups at the C-5 position in both C-6 ester and C-6 amide series generally afforded the potent inhibitors of VEGFR-2 kinase activity and VEGF-stimulated human umbilical vein endothelial cell (HUVEC) proliferation[5] (Table 2). An alkoxy group at the C-5 position (**22**) led to a 6-fold loss in biochemical potency, possibly due to a hydrogen bond between the adjacent aniline NH with the ether oxygen leading to an unfavorable orientation of the aniline. A bulky substituent, such as a *tert*-butyl group at C-5 (**24**) reduced the biochemical potency considerably. In the ester series, both *n*-propyl and

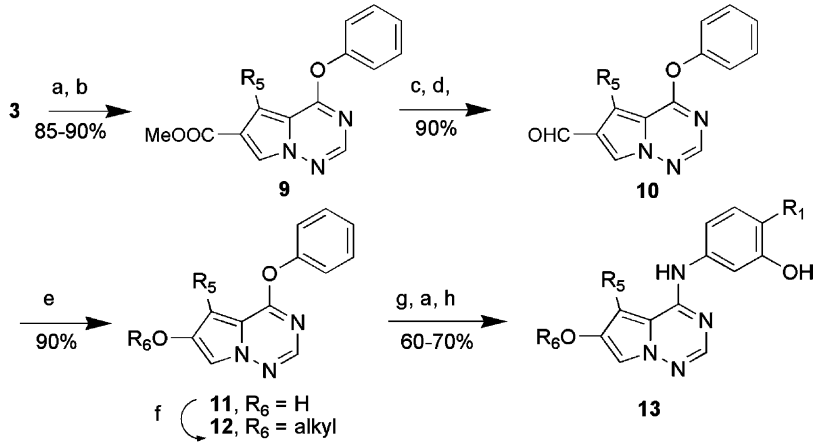

Scheme 2. Synthesis of C-6 ethers. Reagents: (a) $POCl_3$; (b) sodium phenoxide; (c) LAH; (d) MnO_2, toluene, heat; (e) *m*CPBA; (f) R_6Br, NaH or R_6–OH, PPh_3, DEAD; (g) HCl; (h) aniline, CH_3CN, heat.

Table 1. SAR of the aniline ring

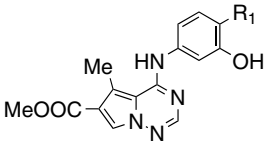

Compd	R_1	VEGFR-2 IC_{50}, nM[a]
14	H	61
15	Me	10
16	Et	55
17	*n*-Pr	190
18	*i*-Pr	380
19	CF_3	370
20	Br	33

[a] For assay conditions see Ref. 5.

Table 2. SAR at C-5 position of pyrrolotriazine

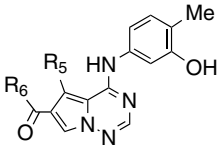

Compd	R_5	R_6	VEGFR-2 IC_{50}, nM[a]	HUVEC[b] IC_{50}, nM
21	*n*-Pr	–OEt	3	6
22	OEt	–OEt	64	40
23	*i*-Pr	–OEt	14	4
24	*t*-Bu	–OMe	310	NA
25	Me	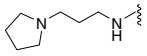	40	10
26	*n*-Pr	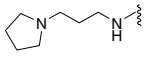	90	35
27	*i*-Pr	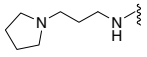	18	8

[a] For assay conditions see Ref. 5.
[b] Human umbelical vein endothelial cells stimulated by VEGF.

i-propyl groups at the C-5 position afforded excellent potency, however, in the metabolically more stable amide series, only the *i*-propyl group maintained acceptable potency and was used in the further SAR.

To better understand the binding mode of these inhibitors, a binding model of **23** in the ATP site of VEGFR-2 was built using the reported crystal structure of the VEGFR-2 kinase domain.[11] Figure 2 depicts the proposed binding mode of **23** in the ATP binding pocket, a model consistent with the reported binding of similar kinase inhibitors.[12]

Key interactions include hydrogen bonds between the N1 nitrogen of the pyrrolotriazine ring and the backbone NH of Cys919 as well as between the phenol OH group and residues Asp1046 and Lys868 in protein kinase ATP-binding pockets. These interactions could potentially be exploited to design pharmacophores that would exhibit better pharmacokinetic properties. The C5-isopropyl group occupies a hydrophobic cleft created by Leu840 and Leu1035 (not labeled in Fig. 2), which also represents the pocket occupied by the ribose ring of ATP. The buried hydrophobic surface areas of both the ligand and protein in this region may account for the increased binding affinity observed in this series

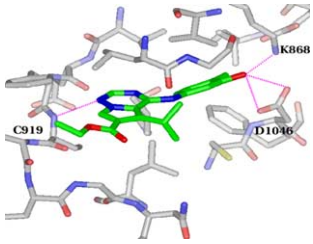

Figure 2. Binding model of **23** in ATP binding site of VEGFR-2 kinase.

relative to unsubstituted analogs.[5] The ester group of **23** points toward surface-exposed protein and longer appendages (**27**) at this position appear to be largely surrounded by solvent. As such the C-6 position affords an opportunity to incorporate moieties that may optimize ADME properties without sacrificing potent binding.

Preliminary in vitro stability testing revealed that early leads suffered from high rates of in vitro metabolism due to facile glucuronidation at the phenol oxygen. Our SAR efforts, therefore, were directed at finding substitutions that would suppress the conjugation reaction. The solvent exposed C-6 position of the pyrrolotriazine was considered to be the most suitable for such a study. Analogs with various appendages attached via different functional groups such as amides, carbamates, ethers, and ureas at the C-6 position were prepared and a possible interplay of substituents at C-5, and C-6 positions on enzymatic activity and in vitro glucuronidation[9] was studied. It was observed that the compounds with neutral groups (**28**–**30**, basic pK_a < 6) exhibited high rates of glucuronidation as shown in Table 3. However, introduction of a basic amino group (calculated basic pK_a between 7 and 10) on an appendage attached to the C-6 position via different groups led to a substantial decrease in the rate of glucuronidation. Thus, the in vitro glucuronidation in human liver microsomes was reduced from 21% in 10 min for **29** to 1% in 10 min for **25**. Similarly, compounds **27**, **31**–**34** also exhibited much lower rates of glucuronidation compared compounds **28**–**30**. At present, it is not clear why a basic group distant from the phenol group mitigates the conjugation reaction.

The effect of the size of the alkyl group at C-5 was minimal (compare **25** and **27**) but carbamates appeared to have higher rates of conjugation compared to the amides, ethers, and ureas (compare **29** with **30** and **31** with **32**).[10]

Despite the very low rates of in vitro glucuronidation and good overall metabolic stability in liver microsomes, these compounds did not exhibit good in vivo pharmacokinetic properties. For example, when administered orally to fasted mice at 50 mg/kg, **27** (in vitro metabolic rate of 0.01 nmol/min/mg at 10 μM of substrate in liver microsomes) demonstrated poor exposure, with C_{max} = 166 nM and $AUC_{0-4\,h}$ = 267 nM h. When dosed iv, high hepatic clearance and a short half-life of 30 min was observed for this compound.

In summary, we report that compounds based on the pyrrolo[2,1-*f*][1,2,4]triazine nucleus containing a 3-hydroxyphenylamino at C-4 and various substituents

Table 3. Optimization of potency and the rate of glucuronidation

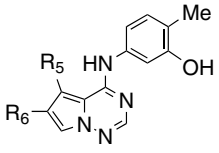

Compd	R_5	R_6	VEGFR-2 IC_{50}, nM[a]	HUVEC[b] IC_{50}, nM	Glucurdn,[c] nmol/min/mg
28	Me	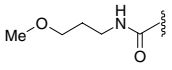	150	ND[d]	0.16
29	Me	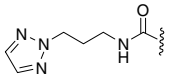	30	20	0.21
30	*i*-Pr	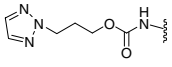	7	ND	0.90
25	Me	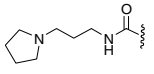	40	10	0.01
27	*i*-Pr	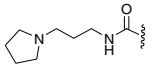	18	8	0.02
31	*i*-Pr	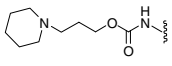	5	1	0.08
32	*i*-Pr	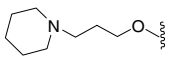	4	1	0.03
33	Me	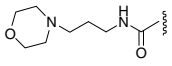	52	3	0.01
34	*i*-Pr	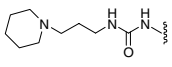	5	5	0.04

[a] For assay conditions see Ref. 5.
[b] Human umbelical vein endothelial cells stimulated by VEGF.
[c] Ref. 9.
[d] Not determined.

at C-6 of the pyrrolotriazine afford VEGFR-2 inhibitors with potent cellular activity. Introduction of a basic moiety at the C-6 position of these phenylamino based inhibitors, while maintaining the biochemical potency, led to a reduction in the in vitro rate of glucuronidation of the phenol. Despite this success, the pharmacokinetic properties of these inhibitors precluded their further development. The versatile synthesis of substituted pyrrolotriazines, the SAR elaborated in this series and the understanding gained from modeling studies, could be helpful in rapid SAR development of a new series possessing improved pharmacokinetic properties.

Acknowledgements

Microanalyses, IR spectra and mass spectra were kindly provided by the Bristol-Myers Squibb Department of Analytical Research and Development. We are grateful to Dr. Louis Lombardo for helpful discussions in the preparation of this manuscript.

References and notes

1. (a) Folkman, J. *Nat. Med.* **1995**, *1*, 27–31; (b) Carmeliet, P.; Jain, R. K. *Nature* **2000**, *407*, 249–257.
2. (a) Robinson, D. R.; Wu, Y. M.; Lin, S. F. *Oncogene* **2000**, *19*, 5548–5557; (b) Jakeman, L. B.; Winer, J.; Bennett, G. L.; Altar, C. A.; Ferrara, N. *J. Clin. Invest.* **1992**, *89*, 244–253.
3. Kim, D. W.; Lu, B.; Hallahan, D. E. *Curr. Opin. Invest. Drugs* **2004**, *5*, 597–604.
4. (a) Yang, J. C.; Haworth, L.; Sherry, R. M.; Hwu, P.; Schwartzentruber, D. J.; Topalian, S. L.; Steinberg, S. M.; Chen, H. X.; Rosenberg, S. A. *New Engl. J. Med.* **2003**, *349*, 427–434; (b) Hurwitz, H.; Fehrenbacher, L.; Novotny, W.; Cartwright, T.; Hainsworth, J.; Heim, W.; Berlin, J.; Baron, A.; Griffing, S.; Holmgren, E.; Ferrara, N.; Fyfe, G.; Rogers, B.; Ross, R.; Kabbinavar, F. *New Engl. J. Med.* **2004**, *350*, 2335–2342.
5. (a) Hunt, J. T.; Mitt, T.; Borzilleri, R.; Gullo-Brown, J.; Fargnoli, J.; Fink, B.; Han, W.-C.; Mortillo, S.; Vite, G.; Wautlet, B.; Wong, T.; Yu, C.; Zheng, X.-P.; Bhide, R. *J. Med. Chem.* **2004**, *47*, 4054–4059; (b) 2.5 μM ATP concentration was used in the enzyme assay.
6. For the detailed experimental see: Hunt, J. T.; Bhide, R. S.; Borzilleri, R. M.; Qian, L. PCT Int. Appl. WO 2000071129.
7. An alternate synthesis of pyrroles **2** could be accomplished using the published route: Suzuki, M.; Miyoshi, M.; Matsumoto, K. *J. Org. Chem.* **1974**, *39*, 1980.
8. Klötzer, W.; Baldinger, H.; Karpitschka, E.-M.; Knoflach, J. *Synthesis* **1982**, 592.
9. The rate of glucuronidation was determined under the following conditions: substrate concentration, 20 μM; protein concentration, 2 mg/mL; UDPGA, 5 mM; pH 7.5 Tris buffer, 100 mM; magnesium chloride, 10 mM; alamethicine (in ethanol), 2.5 μg/mL. Incubations were performed at 37 °C and were initiated by the addition of UDPGA. 200 μL aliquots were taken at times 0, 10, and 20 min and the reaction terminated by the addition of equal volume of acetonitrile. Following vortexing and centrifugation, 20 μL aliquot was analyzed by HPLC-UV. The percentage of compound remaining at each time point was calculated and compared to the values at zero time point. The rate of metabolism was calculated by determining the nanomoles of compound that disappeared and dividing it by the time of incubation and the milligram of protein.
10. ^{1}H NMR (CD_3OD, 300 MHz) of compound **27**: δ 7.80 (s, 1H), 7.55 (s, 1H), 7.01 (d, 1H, J = 8 Hz), 6.77 (s, 1H), 6.64 (d, 1H, J = 8 Hz), 3.60–3.47 (m, 3H), 3.29–3.26 (m, 2H), 3.12–3.10 (m, 2H), 3.08–2.89 (m, 2H), 2.04 (s, 3H), 1.99–1.95 (m, 2H), 1.891.82 (m, 3H), 1.32 (d, 6H, J = 7 Hz).
11. McTigue, M. A.; Wickersham, J. A.; Pinko, C.; Showalter, R. E.; Parast, C. V.; Tempczyk-Russell, A.; Gehring, M. R.; Mroczkowski, B.; Kan, C.-C.; Villafranca, J. E.; Appelt, K. *Structure* **1999**, *7*, 319.
12. Shewchuk, L.; Hassell, A.; Wisely, B.; Rocque, W.; Holmes, W.; Veal, J.; Kuyper, L. *J. Med. Chem.* **2000**, *43*, 133.